JPET Fast Forward. Published on September 2, 2011 as DOI: 10.1124/jpet.111.185348

Therapeutic potential of pegylated hemin for ROS-related diseases via induction of heme oxygenase-1: results from a rat hepatic ischemia/reperfusion injury model

Jun Fang,[1] Haibo Qin,[1] Takahiro Seki,[2] Hideaki Nakamura, Kenji Tsukigawa, and Hiroshi Maeda

Laboratory of Microbiology and Oncology, Faculty of Pharmaceutical Sciences, Sojo University, Kumamoto 860-0082, Japan (JF, HQ, TS, HN, KT); Department of Applied Microbial Technology, Faculty of Biotechnology and Life Science, Sojo University (HQ); DDS Research Institute, Sojo University (HN, HM).

Running title: Pegylated hemin: therapy for ROS-related diseases

Correspondence: Professor Hiroshi Maeda, DDS Research Institute, Sojo University, Kumamoto 860-0082, Japan. Tel: +81-96-326-4114; Fax: +81-96-326-3158; Email: hirmaeda@ph.sojo-u.ac.jp

Number of text pages: 49

Number of tables: 1

Number of figures: 10

Number of references: 42

Number of words in the Abstract: 196

Number of words in Introduction: 712

Number of words in Discussion: 1806

Abbreviations: EPR effect, Enhanced Permeability and Retention effect; ROS, reactive oxygen species; I/R, ischemia/reperfusion.

Recommended Section: Drug Discovery and Translational Medicine

JPET Fast Forward. Published on September 2, 2011 as DOI: 10.1124/jpet.111.185348
This article has not been copyedited and formatted. The final version may differ from this version.

Abstract

Many diseases and pathological conditions including ischemia/reperfusion (I/R) injury are the consequence of the actions of reactive oxygen species (ROS). Controlling ROS generation or its level may thus hold promise as a standard therapeutic modality for ROS related diseases. Here, we assessed heme oxygenase-1 (HO-1), which is a crucial antioxidative, antiapoptotic molecule against intracellular stresses, for its therapeutic potential via its inducer hemin. To improve the solubility and *in vivo* pharmacokinetics of hemin for clinical applications, we developed a micellar hemin by conjugating it with poly(ethylene glycol) (PEG): PEG-hemin. PEG-hemin showed higher solubility in water and significantly prolonged plasma half-life than free hemin, which resulted from its micellar nature with molecular mass of 126 kDa in aqueous media. In a rat I/R model, administration of PEG-hemin significantly elevated HO-1 expression and enzymatic activity. This induction of HO-1 led to significantly improved liver function, reduced apoptosis and thiobarbituric acid reactive substances (TBARS) of the liver, and decreased inflammatory cytokine production. PEG-hemin administration also markedly improved hepatic blood flow. These results suggest that PEG-hemin exerted a significant cytoprotective effect against I/R injury in rat liver by inducing HO-1 and thus appears potential therapeutic for ROS-related diseases including I/R

JPET Fast Forward. Published on September 2, 2011 as DOI: 10.1124/jpet.111.185348
This article has not been copyedited and formatted. The final version may differ from this version.

injury.

Introduction

All aerobic organisms generate reactive oxygen species (ROS), which seem to be indispensable for signal transduction pathways that regulate cell growth and redox status (Davies, 1995). However, overproduction of these highly reactive metabolites can initiate lethal chain reactions and damage cell integrity and survival (Davies, 1995, Oda et al., 1989), which result in reversible and irreversible tissue injury. ROS are known to be involved in many diseases, for example, microbial infections, inflammation, ischemia/reperfusion (I/R) injury, neurological disorders, Parkinson's disease, hypertension, and cancer (McCord, 2000; Maeda and Akaike, 1991). Developing therapeutics for these ROS-related diseases by suppressing ROS generation or its levels in the body therefore seems to be a reasonable approach. Indeed, many research groups have utilized this rationale and investigated various antioxidative agents and enzymes, such as superoxide dismutase (SOD) and catalase (Oda et al., 1989; Muzykantov et al., 1996; Fang et al., 2009a). Inhibitors of the ROS-generating enzyme, xanthine oxidase (XO), were also the targets along this line (Fang et al., 2009a; Miyamoto et al., 1996; Fang et al., 2009b; Fang et al., 2010).

In addition to these enzymes, heme oxygenase-1 (HO-1), the antioxidative, antiapoptotic molecule, has attracted great attention. HO is the key enzyme in heme degradation, which

generates biliverdin, carbon monoxide (CO), and free iron (Fe^{2+}) (Maine, 1988; Fang et al., 2004). Biliverdin is subsequently reduced by cytosolic biliverdin reductase to form bilirubin, a potent antioxidant (Baranano et al., 2002). In addition, recent reports showed CO contributes in regulating vascular tone, and also exhibits antioxidative, anti-inflammatory, and antiapoptotic properties (Abraham and Kappas, 2008). HO-1 is the inducible form of HO, which is a member of the heat shock protein family (Hsp32), and its expression is believed to be associated with fundamental adaptive and defensive responses to oxidative stress and cell stress (Doi et al., 1999; Fang et al., 2004; Abraham and Kappas, 2008). Therefore, induction of HO-1 may become an effective therapeutic strategy for ROS-related diseases. Among HO-1 inducers, hemin is one of the most potent and has few adverse effects to the host. In fact, hemin is used to treat acute hepatic porphyria in Europe and the United States.

However, the very poor water solubility of hemin makes it difficult to achieve a clinically effective dose and develop an optimal therapeutic protocol. To overcome this drawback, we prepared water-soluble micellar form of hemin by using the biocompatible polymer poly(ethylene glycol) (PEG): PEG-hemin. This polymer conjugation resulted in an increased *in vivo* half-life ($t_{1/2}$), and reduced antigenicity, as reported previously (Sawa et al., 2000; Fang et al., 2003), and improves pharmacological efficacy significantly.

I/R injury, a typical ROS-related pathological process, is a major cause of organ damage in many fatal diseases such as cardiac infarction, cerebral ischemia, and thrombosis, as well as in surgical procedures. Many studies reported that ROS, especially superoxide anion radical (O_2^-), is produced excessively in many tissues, mostly by XO, during I/R injury (McCord, 1985). Under normal conditions most of XO is present as xanthine dehydrogenase (type D) (XD), which has very low O_2^--generating activity; however, during ischemia, XO (type O) activity rapidly increases by conversion from XD, which leads to rapid production of O_2^- (Roy and McCord, 1983). O_2^-, with highly cytotoxic activity, is converted to H_2O_2 by SOD, and then to hydroxyl radicals in the presence of transition metals (e.g., Fe^{2+}), if no catalase is available. All these ROS can readily cross cell membranes and cause oxidative damage to DNA, proteins, and lipids (Halliwell and Gutteridge, 1984; Beckman and Ames, 1997; Berlett and Stadtman, 1997). In addition, O_2^- can react rapidly with NO and form the more toxic species peroxynitrite ($ONOO^-$), which further exacerbates tissue injury or leads to complications. Furthermore, removal of NO by reactions with O_2^- on the vascular endothelial surface results in vasoconstriction (hypertension), and triggers neutrophil adherence and accumulation, which will exacerbate reperfusion injury (Beckman and Koppenol, 1996; Akaike and Maeda, 2000). All these data together indicate that ROS are the major cause of

I/R-induced tissue injury and subsequent pathological manifestations.

The present study describes the synthesis of PEG-hemin and the physicochemical and biological characteration of the conjugate. In view of the therapeutic potential of this agent for ROS-related diseases, this study also evaluated the cytoprotective effect of PEG-hemin *in vivo* in a rat liver I/R model.

Materials and methods

Materials

Hemin was purchased from Sigma-Aldrich Chemical Co. (St. Louis, MO). The succinimidyl glutarate derivative of PEG (MEGC-50HS), with a mean molecular weight of 5250, was from NOF Co. (Tokyo, Japan). PEG used in this experiment had a molecular weight dispersity index (Mw/Mn) of 1.025. Other chemicals of reagent grade were from Wako Pure Chemical Industries Ltd. (Osaka, Japan) and were used without additional purification.

Cell culture

Human hepatocyte Hc cells (DS Pharma Biomedical Co. Ltd, Osaka, Japan) were cultured in CSC Serum-Free Medium (DS Pharma) at 37°C in a 5% CO_2/95% air atmosphere.

Animals

Male Wistar rats, 6-7 wk old and weighing between 200 and 230 g, and 6-wk-old male ddY mice weighing between 20-25 g were obtained from Kyudo Inc. (Kumamoto, Japan). All animals were maintained under standard conditions and were fed water and murine chow *ad libitum*. All experiments were carried out according to the guidelines of the Laboratory Protocol of Animal Handling, Faculty of Pharmaceutical Sciences, Sojo University.

Synthesis of PEG-hemin

PEG-hemin was synthesized according to the protocol for PEG-zinc protoporphyrin (PEG-ZnPP) synthesis described in our previous work (Sahoo et al., 2002), with some modifications. Briefly, an aminated derivative of hemin was synthesized by using ethylenediamine, and then succinimidyl PEG was cross-linked to hemin via the amide bond (Scheme 1). The resultant PEG-hemin was characterized by means of a UV spectrophotometer (Model UV/Vis-550; JASCO Corp., Tokyo, Japan) and infrared spectrometer (FT/IR-4200; JASCO), as well as dynamic light scattering (DLS) and Sephadex column chromatography, as described below.

Quantification of the free amino group

To determine whether PEG reacted with the amino group introduced into hemin, loss of the primary amino group after the reaction was quantified by use of fluorescamine, an amino

JPET Fast Forward. Published on September 2, 2011 as DOI: 10.1124/jpet.111.185348
This article has not been copyedited and formatted. The final version may differ from this version.

group-reactive fluorescent agent (Stocks et al., 1986). Briefly, 2 μM PEG-hemin (hemin equivalent) and diethylaminohemin (aminated derivative of hemin) were dissolved in deionized water and then reacted with fluorescamine. Fluorescence was detected at 475 nm with excitation at 390 nm. The concentration of free amino groups in PEG-hemin was estimated by using glycine as the standard.

Size exclusion chromatography

Size exclusion chromatography was performed with a Sephadex G-100 column, 40 cm (length) × 1.3 cm (diameter) (Pharmacia LKB, Uppsala, Sweden), to determine the apparent molecular mass of PEG-hemin. Various globular proteins of known molecular mass were used as reference standards. The mobile phase was 0.25 M $NaHCO_3$ (pH 8.2), and 2.5-ml fractions were collected per tube.

DLS measurement of PEG-hemin particle size

DLS measurement was performed with the Photal DLS-7000 HLs laser spectrophotometer (Otsuka Electronics, Osaka, Japan), equipped with a 10-mW He/Ne laser, at a wavelength of 632.8 nm. The scattering angle was fixed at 90° and the temperature at 25°C ± 0.05°C. Particle size was determined with 0.1 mg/ml samples prepared in deionized water (filtered through a 0.45 μm filter).

JPET Fast Forward. Published on September 2, 2011 as DOI: 10.1124/jpet.111.185348
This article has not been copyedited and formatted. The final version may differ from this version.

***In vivo* pharmacokinetics of PEG-hemin**

ddY mice were used in the determination of PEG-hemin plasma $t_{1/2}$, area under the concentration *vs.* time curve (AUC), and total body clearance. PEG-hemin (dissolved in physiological saline) or free hemin (dissolved in 0.01 M NaOH with 10% DMSO) was injected intravenously (i.v.) at 10 mg/kg (hemin equivalent). After scheduled intervals, mice were killed and blood was collected in the presence of heparin, so that plasma could be obtained after centrifugation at 5000 *g* for 20 min at 4°C. Then, to 0.2 ml of plasma 1.8 ml of ethanol with 0.25 M HCl was added, to extract PEG-hemin or hemin. After vigorous vortexing and centrifugation at 20,000 *g* for 20 min, supernatant UV spectra between 300 and 600 nm were measured, and peak absorbance at 385 nm was utilized to calculate the concentration of hemin according to the standard curve of hemin.

***In vitro* cytotoxicity assay of PEG-hemin**

Human hepatocytes (Hc) were plated at 3000 cells/well in a 96-well plate (Nunc A/S, Roskilde, Denmark). After overnight preincubation, different concentrations of PEG-hemin were added to the cells. After an additional 48 h incubation, cell viability was determined by using the MTT assay (Dojindo Laboratories, Kumamoto, Japan).

Induction of HO-1 expression in human hepatocytes by PEG-hemin

To investigate the HO-1-inducing activity of PEG-hemin, HO-1 expression in human hepatocytes (Hc) was determined with or without PEG-hemin treatment. Hc cells were plated in 6-well culture plates (50,000 cells/well), incubated overnight at 37^{o}C, and treated with indicated concentrations of PEG-hemin for 24 h. Cells were then collected, and total RNA and protein were extracted by using TRIzol reagent (Life Technologies, Inc., Grand Island, NY) and CelLytic MT (Sigma) reagent, according to the manufacturers' instructions. RT-PCR was performed for quantification of HO-1 copies in Hc Cells. Primers used for PCR were as follows: HO-1 antisense 21-mer, 5′GATGTTGAGCAGGAACGCGAT3′, and HO-1 sense 21-mer, 5′CAGGCAGAGAATGCTGAGTTC3′, to obtain a 555-bp HO-1 cDNA (nucleotides 79 to 633); and GAPDH antisense 24-mer, 5′CATGTGGGCCATGAGGTCCACCAC3′, and sense 26-mer, 5′TGAAGGTCGGAGTCAACGGATTTGGT3′, to obtain a 983-bp GAPDH cDNA fragment. After an initial denaturing step at 94°C, 25 PCR cycles (30 cycles for GAPDH) were performed as follows: denaturing for 1 min at 94°C, primer annealing for 1 min at 56°C, and DNA synthesis for 1 min at 72°C. PCR products then underwent electrophoresis on ethidium bromide-stained 1% agarose gels.

Experimental protocol for hepatic I/R injury

Rats were fasted overnight before the experiment but were allowed free access to water.

Animals were anesthetized with isoflurane during the operation by using an anesthesia system (SF-B01; DS Pharma Biomedical Co. Ltd). After the abdomen was shaved and disinfected with 70% ethanol, a complete midline incision was performed. The portal vein and hepatic artery were exposed and were cross-clamped for 30 min with a noncrushing microvascular clip. Subsequently, reperfusion was initiated by removing the clips, and the abdomen was closed in two layers with 2-0 silk. Rats were kept warmed until they awoke and became active. Two hours before surgery for I/R, saline or PEG-hemin at different doses (2, 10 mg/kg) was injected into each rat via the tail vein. In some experiments, a polymeric micellar HO-1 inhibitor, zinc protoporphyrin (ZnPP) encapsulated with styrene maleic acid (SMA) copolymer, namely SMA-ZnPP (Iyer et al., 2007), was administered i.v. (5 mg/kg) just before I/R.

Measurement of liver enzyme activity in serum

Three hours after reperfusion resumed, rats were killed under anesthesia, and whole blood was withdrawn from the inferior vena cava. Activities of alanine aminotransferase (ALT), aspartate aminotransferase (AST), and lactate dehydrogenase (LDH) in serum were determined by means of the AutoAnalyzer system (Hitachi Ltd., Tokyo, Japan). Activities were expressed as international units per liter (IU/L).

Measurement of HO-1 expression and activity in rat liver after I/R

Liver tissues collected from rats receiving the above-described treatment with PEG-hemin or no treatment were homogenized with the Polytron homogenizer (Kinematica Inc., Littau-Lucerne, Switzerland) in ice-cold homogenizing buffer [20 mM potassium phosphate buffer (pH 7.4) plus 250 mM sucrose, 2 mM EDTA, 2 mM phenylmethylsulfonyl fluoride, and 10 μg/ml leupeptin]. Homogenates were centrifuged at 10,000 *g* for 30 min at 4°C, and the resultant supernatant was ultracentrifuged at 105,000 *g* for 1 h at 4°C. The microsomal fraction in the precipitates was suspended in 0.1 M potassium phosphate buffer (pH 7.4) followed by sonication for 2 s at 4°C.

Supernatant of the 10,000 *g* fraction, with 50 μg of protein in each sample, was used for analysis of HO-1 expression by Western blot. In brief, total protein were separated by electrophoresis with 12% sodium dodecyl sulfate (SDS)-polyacrylamide gels and were transferred to Immobilon polyvinylidene difluoride membranes (Millipore Co., Ltd., Bedford, MA, USA). This process was followed by reaction with a monoclonal antibody for HO-1 (GTS-1; Takara Bio Inc., Otsu, Shiga, Japan). The protein band that reacted immunologically with the antibodies was visualized by using the enhanced chemiluminescence system (Amersham International Plc, Burk, UK).

The microsomal fraction was used for measurement of HO-1 activity. The HO reaction

JPET Fast Forward. Published on September 2, 2011 as DOI: 10.1124/jpet.111.185348
This article has not been copyedited and formatted. The final version may differ from this version.

mixture consisted of the microsomal fraction (1 mg of protein), cytosolic fraction (supernatant after ultracentrifugation described above) of rat liver (1 mg of protein) as a source of biliverdin reductase, 33 μM hemin, and 333 μM NADPH in 1 ml of 0.1 M potassium phosphate buffer (pH 7.4). The mixture was incubated for 15 min at 37°C, after which the reaction was terminated by addition of 33 μl of 0.01 M HCl. Bilirubin formed in the reaction was extracted with 1.0 ml of chloroform, and bilirubin concentration was determined spectroscopically by measuring the difference in absorbance between 465 nm (absorbance of bilirubin) and 530 nm (background), with a molar extinction coefficient of 40 mM^{-1} cm^{-1} at 465 nm.

Moreover, HO-2 expression in this experimental protocol was measured by RT-PCR. In brief, total RNA of each liver tissue was extracted by using TRIzol reagent (Life Technologies, Inc.,) according to the manufacturers' instructions. Primers used for PCR were as follows: antisense, 5′ AGTAAAGTGCAGTGGTGGCC3′, and sense, 5′ 5-CAGCAACAATGTCTTCAGAGG3′ to obtain a 230-bp HO-2 cDNA. After an initial denaturing step at 94°C, 35 PCR cycles were performed as follows: denaturing for 2 min at 92°C, primer annealing for 1 min at 54°C, and DNA synthesis for 1 min at 72°C. PCR products then underwent electrophoresis on ethidium bromide-stained 1% agarose gels.

Quantification of CO in blood

After the I/R procedure just described, rats were killed and blood was collected. Each 0.35 ml sample of blood was diluted with 3.65 ml of phosphate-buffered saline and placed in a 10 ml glass test tube on ice. The test tubes were then sealed, and the air in the tubes was replaced by purging nitrogen gas into the tubes, after which the NO donor NOC-7 [3-(2-hydroxy-1-methyl-2-nitrosohydrazino)-*N*-methyl-1-propanamine] was added, to a final concentration of 1 mM. Because NO has a much higher affinity than CO for hemoglobin, CO bound to hemoglobin would be liberated. After 2 h of incubation at room temperature, 1 ml of the gas in the test tubes was collected and processed in a gas chromatography CO analyzer (TRIlyzer mBA-3000; TAIYO Instruments, Inc., Osaka, Japan) equipped with a semiconductor gas sensor.

Preparation of liver tissue sections for histological examination and detection of apoptosis

Rat livers were collected 3 h after I/R and were cut into small tissue blocks (about 3-5 mm in length, width and height). After the blocks were fixed with 6% buffered neutral formalin solution, they were embedded in paraffin. Paraffin-embedded sections (6 μm thick) were prepared as usual for histological examination after hematoxylin and eosin (H&E) staining and for apoptosis staining (TUNEL) as described below.

JPET Fast Forward. Published on September 2, 2011 as DOI: 10.1124/jpet.111.185348
This article has not been copyedited and formatted. The final version may differ from this version.

***In situ* detection of apoptosis in the liver**

TUNEL staining was used to investigate apoptosis in the paraffin-embedded sections described above, after I/R with or without PEG-hemin treatment, with an in situ apoptosis detection kit (TACS; Trevigen Inc., Gaithersburg, MD), according to the manufacturer's instructions. TUNEL-positive cells in four different fields per sample were counted, and results were expressed per mm^2 of tissue section.

Detection of caspase 3/7 activities in the liver

Apoptosis in the livers of different treatment groups were further examined in their caspase 3/7 activities, with a caspase assay kit which contains the substrate peptide DEVD (Caspase-Glo 3/7 Assay, Promega Co., Madison, WI). Briefly, the liver tissue homogenates were prepared by using 1 g of wet tissue adding with 4 ml of hypotonic extraction buffer [25 mM HEPES buffer (pH 7.5), 5 mM $MgCl_2$, 1 mM EGTA, 2 mM phenylmethylsulfonyl fluoride, and 10 μg/ml leupeptin] with the Polytron homogenizer (Kinematica Inc.). Homogenates were centrifuged at 10,000 *g* for 30 min at 4°C, and the supernatant was used for caspase activity assay according to the manufacturer's instructions.

Measurement of liver tissue blood flow

A laser Doppler flowmeter (ALF21; Advance Co. Ltd., Tokyo, Japan) was utilized to

measure liver tissue blood flow in anesthetized animals during I/R (until 1 h after initiating reperfusion) with or without PEG-hemin treatment (10 mg/kg i.v.). The flowmeter probe was inserted at the same site in the median lobe of the liver in each animal. The real-time change in blood flow was monitored, and the mean blood flow at specific time points was calculated and expressed as a percentage of the preischemic initial blood flow value as the control.

Thiobarbituric acid-reactive substance (TBARS) assay

Oxidative cell damage in the liver after I/R with or without PEG-hemin treatment was quantified by assay of lipid peroxide formation via the thiobarbituric acid (TBA) reaction (Ohkawa et al., 1979). Briefly, liver tissue homogenates were prepared at a ratio of 1 g of wet tissue to 9 ml of 1.15% KCl in a Polytron homogenizer. Then, 0.1 ml of homogenate was mixed with 0.2 ml of 8.1% SDS, 1.5 ml of 20% acetic acid (pH 3.5 adjusted with NaOH), and 1.5 ml of a 0.8% aqueous solution of TBA. The final sample was made up to 4 ml with distilled water and incubated at 95°C for 60 min. After cooling with tap water, 1.0 ml of distilled water and 5.0 ml of a mixture of *n*-butanol and pyridine (15:1, v/v) were added, and each reaction mixture was shaken vigorously. After centrifugation at 5000 *g* for 10 min, absorbance of the organic upper layer was measured at 532 nm.

ELISA for 8-OHdG (8-hydroxydeoxyguanosine) in the liver

JPET Fast Forward. Published on September 2, 2011 as DOI: 10.1124/jpet.111.185348
This article has not been copyedited and formatted. The final version may differ from this version.

Oxidative injury of the liver after I/R with or without PEG-hemin treatment was further examined by detecting 8-OHdG in liver tissues, by use of an ELISA kit (8-OHdG Check, JalCA, Fukuroi, Shizuoka, Japan). In brief, DNA in each sample was extracted by using QuickGene DNA tissue kit (DT-S, Wako Ltd.), followed by hydrolysis using an 8-OHdG Assay Preparation Reagent Set (Wako Ltd.). The ELISA assay was then performed to detect 8-OHdG according to he manufacturer's instructions.

ELISA for monocyte chemotactic protein (MCP)-1 in serum

Serum samples from I/R-treated rats were obtained as described above, and the MCP-1 levels were quantified by using an ELISA kit (Immuno-Biological Laboratories Co., Ltd., Takasaki-Shi, Gunma, Japan) according to the manufacturer's instructions.

Statistical analysis

All data are expressed as means ± SE. Student's *t* test was used to determine the significance between each experimental group. A difference was considered statistically significant when $P < 0.05$.

Results

Synthesis of PEG-hemin

As we reported previously, to facilitate conjugation of hemin with PEG we first conjugated with ethytlenediamine to generate amino groups onto two carboxyl groups in the porphyrin ring of hemin, to produce more reactive nucleophiles than the original carboxyl group (Sahoo et al., 2002). Then, pegylation targeted to the amino groups was successfully achieved by using succinimidyl-activated PEG, with two PEG chains conjugated to the porphyrin structure of hemin (Scheme 1). The resulting PEG-hemin exhibited a high water solubility, more than 15 mM, whereas native hemin is almost insoluble in water or physiological solutions. Physiochemical analysis showed that PEG-hemin had a UV spectrum that was similar to that of free hemin (data not shown). IR spectra of PEG-hemin exhibited a characteristic absorption of amide bonds at 1654 cm^{-1} (amide I) and 1542 cm^{-1} (amide II) (Fig. 1), which demonstrated conjugation between PEG and hemin via amide bonds. Crosslink of PEG was further supported by the fact that PEG-hemin had no free amino groups after pegylation (Scheme 1), as determined by fluorescamine (data not shown).

The molecular mass of PEG-hemin, as calculated from the chemical structure of PEG-hemin shown in Scheme 1, was 10-12 kDa with two PEG molecules (about 5000 Da each) conjugated per mole of hemin. However, in aqueous solutions, PEG-hemin had a large molecular mass, approximately 126 kDa as analyzed by Sephadex G-100 column

chromatography (Fig. 2A). This result was confirmed by DLS, which showed a mean particle size of 121.5 nm in deionized water (Fig. 2B). The particle size of PEG-hemin in water remained unchanged at 4°C for more than 1 month. These data clearly indicated the formation of stable micelles of PEG-hemin in aqueous solution, with the hydrophobic core assembly of hemin inside and the hydrophilic PEG outside (Scheme 1).

Plasma $t_{1/2}$ of PEG-hemin

We expected the macromolecular micellar formulation of PEG-hemin to have superior *in vivo* pharmacokinetics (e.g., prolonged $t_{1/2}$), and we investigated this possibility by using ddY mice. Compared with free hemin, PEG-hemin had a relatively long circulation time: even 20 h after i.v. injection, about 30% remained in circulation; almost no hemin was detected 2 h after administration (Fig. 3). The $t_{1/2}$ of PEG-hemin was calculated to be 18.2 h, which is about 20 times longer than that of hemin (0.96 h); in parallel, the AUC of PEG-hemin increased to 16 times of that of free hemin, and the total body clearance of PEG-hemin was about 16 times slower than that of free hemin (Table 1).

***In vitro* cytotoxicity and HO-1 induction activity of PEG-hemin**

Figure 4A shows no apparent cytotoxicity for PEG-hemin up to 250 μM (hemin equivalent). More important, PEG-hemin treatment significantly induced expression of HO-1

mRNA in cultured human hepatocytes (Fig. 4B).

***In vivo* HO-1 induction by PEG-hemin in a rat liver I/R model**

I/R procedure alone increased HO-1 protein expression in the liver tissue, but more important, this HO-1 expression was dramatically upregulated by PEG-hemin treatment (Fig. 5A). Similarly, HO-1 activity in liver tissue, as assessed by the production of bilirubin, increased after I/R but more significantly increased after I/R plus PEG-hemin treatment (Fig. 5B). These findings were supported by the PEG-hemin-induced significant increase in the blood concentration of CO, which is another major product of HO-1-catalyzed heme degradation (Fig. 5C).

In addition, I/R procedure induced a slight increase of HO-2 expression, however, PEG-hemin treatment did not affect HO-2 expression (Supplement Figure 1).

Amelioration of liver I/R injury by PEG-hemin

The potential therapeutic or tissue protective effect of PEG-hemin against I/R injury of the liver was evaluated by measuring plasma concentrations of the liver enzymes AST, ALT, and LDH. In our previous study, we reported that these enzymes increased to a maximum level at 3 h after reperfusion (Ikebe et al., 2000); thus, in this study all experiments were performed at 3 h after reperfusion. As anticipated, I/R caused a large increase in levels of all three liver

enzymes, to more than 20 times of normal levels. AST, ALT, and LDH values for I/R vs. those for normal rat were as follows: 2647.4 ± 460.4 IU/L *vs.* 65.3 ± 0.7 IU/L, 1356.4 ± 182.1 IU/L *vs.* 54.3 ± 1.2 IU/L, and 6932.6 ± 1131.0 IU/L *vs.* 62.3 ± 3.4 IU/L, respectively) (Fig. 6A).

More important, PEG-hemin treatment, at 10 mg/kg (hemin equivalent), significantly lowered the elevated levels of AST, ALT, and LDH, with liver enzyme levels almost recovering to normal (Fig. 6A). Furthermor, this cytoprotective effect of PEG-hemin was almost nullified by administration of SMA-ZnPP, which is a macromolecular water-soluble HO inhibitor that we had previously prepared (Iyer et al., 2007) (Fig. 6A). These results suggest that the cytoprotective effect of PEG-hemin was through an HO-1-mediated pathway, as discussed in the Introduction. Consistent with these findings, H&E staining of liver tissues after I/R revealed apparent necrotic areas, but necrosis was significantly inhibited by PEG-hemin treatment (Fig. 6B). In addition, rats not undergoing I/R showed no apparent changes in serum AST, ALT, and LDH values after injection of PEG-hemin (data not shown), which suggests that PEG-hemin seemed to be nontoxic to the liver.

Changes in hepatic blood flow

One major reason for liver tissue injury by I/R is reduced blood flow, as clearly seen in Fig. 7, which shows that hepatic blood flow decreased to 20% of normal at 20 min after ischemia

and recovered to only 30% of normal at 1 h after reperfusion was initiated. The tissue protective effect of PEG-hemin was believed to result, at least in part, from improved hepatic blood flow. PEG-hemin treatment largely increased hepatic blood flow, which reached 80% of normal at 1 h after the start of reperfusion (Fig. 7).

Apoptosis in the liver after I/R

The TUNEL assay for apoptosis allowed further elucidation of the pathological events caused by I/R with or without PEG-hemin treatment. I/R clearly induced apoptosis at 3 h after reperfusion, whereas PEG-hemin significantly lowered the number of apoptotic cells in the liver after I/R (Fig. 8A), findings that correlated well with the liver enzyme profiles. This was further supported by caspase 3/7 activity assay, by which the caspase 3/7 activities were found to be remarkably increased in the livers of I/R, whereas it was significantly inhibited by PEG-hemin (Fig. 8B).

Oxidative injury induced by I/R in the liver

To investigate the role of ROS in liver I/R injury, the TBARS assay, which is a standard method of detecting oxidative injury of tissue involving lipid peroxidation, was performed. As Fig. 9 shows, I/R greatly increased the TBARS level in the rat liver. This increase was markedly inhibited by PEG-hemin treatment, in a dose-dependent manner (Fig. 9): at 10 mg/kg

PEG-hemin, the TBARS value was almost normal, which suggests that liver injury caused by I/R involved the increased generation of ROS. Similar results were obtained when 8-OHdG that is a common index for oxidative injury of DNA, was detected in the liver of rat after I/R procedure with or without PEG-hemin treatment. These findings all together indicate the involvement of ROS in I/R injury and the protective effect of PEG-hemin in this process.

Change in serum inflammatory cytokine MCP-1 level after I/R with or without PEG-hemin

Inflammation is a major consequence of ROS-related diseases and thus plays a crucial role in the pathological process of I/R. Among the many inflammatory cytokines known to be involved in I/R injury, MCP-1, a proinflammatory chemokine and key mediator in the inflammatory process, is strongly associated with ROS-induced pathological conditions including I/R injury (Melgarejo et al., 2009). We thus measured the levels of MCP-1 in rat serum after I/R with or without PEG-hemin administration. Figure 10 shows a significantly increased serum MCP-1 level at 3 h after I/R. However, PEG-hemin treatment before I/R markedly inhibited this increase, which was consistent with the liver function results, as well as necrosis and apoptosis in liver tissue.

Discussion

During the past few decades, the clinical importance of ROS has been discussed extensively, and development of drugs to control the generation of ROS or scavenge ROS, has become a focus of great interest (Maeda and Akaike, 1991; McCord, 2000). One approach is to block ROS generation. We in fact developed an XO inhibitor, AHPP (4-amino-6-hydroxypyrazolo[3,4-*d*]pyrimidine), and its polymer conjugate to inhibit O_2^- production by XO (Miyamoto et al., 1996; Fang et al., 2009b; Fang et al., 2010). An alternative approach that has attracted our attention is to take advantage of the products of HO-1, which is a major antiapoptotic antioxidative molecule (Maines, 1988; Fang et al., 2004; Abraham and Kappas, 2008). Induction of HO-1 either by its inducers such as cobalt protoporphyrin, hemin or by HO-1 gene transfer showed beneficial effects in many ROS-related diseases (Fang et al., 2004; Abraham and Kappas, 2008). We followed this approach using a modified hemin, and developed a macromolecular micellar hemin formulation to improve its water solubility and *in vivo* pharmacokinetics.

We utilized PEG, which is a widely used biocompatible polymer, to prepare hemin micelles. Consistent with our previous reports of PEG-ZnPP (Sahoo et al., 2002; Fang et al., 2003), which is chemically similar to PEG-hemin, PEG modification of hemin led to markedly

JPET Fast Forward. Published on September 2, 2011 as DOI: 10.1124/jpet.111.185348
This article has not been copyedited and formatted. The final version may differ from this version.

increased solubility (more than 15 mM; hemin equivalent) in physiological solutions, in which free hemin can be hardly solubilized. More important, PEG-hemin exhibited a very long circulation time: its $t_{1/2}$ in ddY mice was about 18 h, which was approximately 20 times longer than that of free hemin (Fig. 3, Table 1). Furthermore, PEG-hemin had no or very little toxicity: PEG-hemin treatment, up to 250 μM, produced no cell death (Fig. 4A). Its safety was also verified *in vivo*: injection (i.v.) of 100 mg/kg PEG-hemin into ddY mice did not cause death of the mice, or any apparent side effect such as loss of body weight and change in blood biochemistry (data not shown). These findings warrant further clinical applications of PEG-hemin.

The improved water solubility and plasma $t_{1/2}$ are due to the micellar formulation of PEG-hemin, which had an apparent molecular mass of 126 kDa in aqueous solution as judged by Sephadex G-100 column chromatography (Fig. 2A). This PEG-hemin presents as aggregated micellar form, as observed by DLS, which showed a mean particle size of 121.5 nm in physiological solution (Fig. 2B). Macromolecular drugs (larger than 40 kDa) are known to have various beneficial characteristics including prolonged *in vivo* $t_{1/2}$ as shown above, and, what is more important, selective accumulation and retention in solid tumor and inflammatory tissues. This unique phenomenon of macromolecules was named the enhanced permeability

and retention effect (EPR effect) (Matsumura and Maeda, 1986; Maeda et al., 2000, 2001; Duncan, 2003; Fang et al., 2011). Many macromolecular drugs have been developed on the basis of the EPR effect and are now not only at the laboratory stage of development but also in clinical stage (Maeda et al., 2001; Duncan, 2003; Nagamitsu et al., 2009; Maeda, 2010; Fang et al., 2011).

In addition, the macromolecular PEG-hemin micelles showed relatively strong HO-1 induction activity, both *in vitro* and *in vivo*, as evidenced by mRNA and protein levels (Figs. 4B and 5A). More important was HO-1 enzymatic activity of generation of both antioxidative bilirubin and CO (Fig. 5B, 5C), which are the essential components to exhibit the pharmacological effect of HO-1. By quantifying bilirubin production, one can assess the enzyme activity of HO. However it may not reflect the physiological role of HO *in vivo*. Measurement of CO that is derived mostly from HO in biological organisms (Abraham and Kappas, 2008), in circulation or tissues may thus useful to evaluate the physiological role of HO *in vivo*. The results presented in this study clearly indicated the correlation of the circulation CO level in parallel with HO expression and bilirubin production (Fig. 5). Further investigations are warranted for measurement of CO levels in tissues.

Mechanisms involved in the tissue protective and therapeutic effects of PEG-hemin were

thought to rely mostly on the antioxidative role of HO-1, which would take advantage of the enzyme reactions in heme catabolism (Fang et al., 2004; Abraham and Kappas, 2008). Heme and free iron are pro-oxidants that would induce or enhance ROS generation (Akaike et al., 1992; Jeney et al., 2002), whereas bilirubin, which is a major product of heme degradation, is one of the most abundant endogenous antioxidants in mammals and accounts for the major antioxidative activity in human serum (Baranano et al., 2002).

More recently, CO generated during heme degradation is also believed to account for the major, if not all, biological properties of HO-1. HO-catalyzed heme catabolism is the major source of CO (i.e., more than 80%) in mammalian system, and the roles of CO include, as similar to NO, regulating vascular tone (vasorelaxant), participating in antiapoptosis, serving an antioxidative, anti-inflammatory function and inhibiting the activation of monocyte/macrophages, inducing angiogenesis, and others (Abraham and Kappas, 2008). In our present experiment, we found the CO concentration in circulation increased after PEG-hemin treatment (Fig. 5C) which was paralleled with the improved hepatic blood flow (Fig. 7) and decreased apoptosis in the liver underwent I/R process (Fig. 8), even though we did not show direct evidence of its role on the cytoprotective effect against I/R injury. However, a recent study by Wei and colleagues (Wei et al., 2010) demonstrated a direct effect

of CO on I/R injury by using a CO-releasing molecule, although the effect was less significant, probably because of the short *in vivo* $t_{1/2}$ of CO-releasing agent.

Besides HO-1 (the inducible enzyme), the constitutive form of HO, namely HO-2 is another major source of HO activity in most tissues. Both are alike in terms of enzymatic mechanisms of heme degradation, cofactor and substrate specificity (Maines, 1988; Abraham and Kappas, 2008). The HO activities in liver tissues measured in this study (Fig. 5B) may thus include HO-2 activity as well. Unlike HO-1, whose expression is relatively low in most normal tissues unless exposed to various stresses, such as I/R injury and hemin treatment as shown in this study (Fig. 5), however, HO-2 displays, in general, a constitutive expression in many normal tissues but it is not upregulated upon stress or injury which was also confirmed in this study (Supplement Figure 1). HO-2 is thus believed to contribute to normal housekeeping. And recently, it was reported that HO-2 behaves as a basal tone of anti-inflammatory signals, deletion of HO-2 disables execution of the acute inflammatory and reparative response, leading to an exaggerated inflammatory response including increased oxidative stress and angiogenesis (Seta et al., 2006; Bellner et al., 2009). Moreover, it is known that HO-2 is induced by treatment of corticosteroids (Maines et al., 1996), which is an important protective response during acute illness or stress, and is widely used as a treatment of

inflammatory diseases. Thus, HO-2, along with HO-1, may also play important role as a protective response against I/R as well as inflammatory distress, facilitating the therapeutic response induced by PEG-hemin, which warranted further investigations.

I/R injury is a typical ROS-related inflammatory disorder, in which O_2^-, as a highly reactive radical, reacts with and oxidize many biological molecules including NO (McCord, 1985; Maeda and Akaike, 1991; Ikebe et al., 2000) and thereby can trigger cell death. These pathological roles were clearly demonstrated in the present study using I/R procedure, as evidenced by increased levels of the inflammatory cytokine MCP-1 (Fig. 10), elevated TBARS and 8-OHdG (Fig. 9), and apoptosis in liver tissue (Fig. 8), all of which were at least partly ameliorated by PEG-hemin treatment. As described above, O_2^- reacts extremely rapidly with NO at diffusion rate dependent manner, and NO is thus removed and bioavailability of NO is reduced in the body resulting in vascular constriction. These events explain, at least partly if not completely, the low hepatic blood flow after reperfusion during I/R, as Fig. 7 shows. Scavenging O_2^- will result in the reduction of apoptosis of hepatic cells and improve hepatic blood flow (Figs. 7 and 8), as a consequence, pathological effects due to I/R injury will be prevented.

With regard to the treatment protocol in the present study, PEG-hemin was administered 2

h before ischemia was initiated, so as to achieve sufficient HO-1 induction, as shown in Figure 5. This study utilized an acute I/R injury model, in which the injury peaked within 3 h, so that induction of HO-1 before I/R was necessary; late treatment may be less effective because pathological changes progress quickly and may not be reversed before sufficient HO-1 expression. Acute I/R injury can in fact be observed in many medical interventions, such as routine operations, and especially organ transplantation, in which temporary obstruction of the blood flow of an organ or tissue is necessary, and the I/R injury of the tissue or organ is unavoidable and predictable. In these cases, prior administration of PEG-hemin and induction of HO-1 would be reasonable and practical and may produce successful therapeutic results. However, many I/R injuries seen in clinical settings are subacute or chronic, in which ROS are generated and injury progresses slowly but gradually; these situations include cardiac arrest, cerebral ischemia, thrombosis, and stroke (McCord, 1985). PEG-hemin may thus be beneficial in these cases with its long plasma half-life (Fig. 3, Table 1) and thus potent and sustained HO-1 induction activity. For groups at high risk of developing these diseases, PEG-hemin may become more important as a preventive medication because PEG-hemin itself demonstrated no or very little toxicity (Fig. 4A).

In addition, many disorders other than I/R injury are associated with ROS including

inflammation, hypertension, and bacterial and viral infections (McCord, 2000; Maeda and Akaike, 1991). Therefore PEG-hemin may be applicable for the treatment of these diseases as well.

In conclusion, findings from the present study demonstrated that the macromolecular, water-soluble, micellar form of HO-1 inducer PEG-hemin exerted a potent cytoprotective effect against I/R injury of the liver in rats, as evidenced by low serum liver enzyme values (Fig. 6A), decreased numbers of apoptotic cells in the liver (Fig. 8), increased hepatic blood flow (Fig. 7), and reduced inflammatory cytokine levels in serum (Fig. 10). The cytoprotective effects of PEG-hemin can be attributed to augmented HO-1 activity (e.g., increased CO production, as Fig. 5C showed) through its antiapoptotic, antioxidative actions, because the HO-1 inhibitor SMA-ZnPP almost completely nullified the effect of PEG-hemin (Fig. 6A). This finding was also supported by the increased HO-1 mRNA and protein expression as well as elevated CO levels in blood and HO-1 enzyme activity (Fig. 4B, Fig. 5), and reduced tissue peroxidation in the liver after PEG-hemin treatment (Fig. 9). Therefore, the data presented herein suggest a therapeutic potential of PEG-hemin for I/R injury, as well as other ROS-related diseases, such as inflammatory disorders and hypertension, so that PEG-hemin warrants further investigation as a therapeutic agent.

Acknowledgments

We thank Judith Gandy for editing the manuscript.

Authorship Contributions

Participated in research design: Fang, and Maeda.

Conducted the animal experiments and biological assays: Fang, and Qin.

Contributed to the synthesis and characterization of PEG-hemin: Fang, Qin, Nakamura, and Tsukigawa.

Wrote or contributed to the writing of the manuscript: Fang, Qin, and Maeda.

References

Abraham NG, and Kappas A (2008) Pharmacological and clinical aspects of heme oxygenase. *Pharmacol Rev* **60:** 79-127.

Akaike T, and Maeda H. (2000) Pathophysiological effects of high-output production of nitric oxide, in *Nitric Oxide: Biology and Pathology* (Ignarro LJ ed) pp 733-745, Academic Press, San Diego.

Akaike T, Sato K, Ijiri S, Miyamoto Y, Kohno M, Ando M, and Maeda H. (1992) Bactericidal activity of alkyl peroxyl radicals generated by heme-iron-catalyzed decomposition of organic peroxides. *Arch Biochem Biophys* **294:** 55-63.

Baranano DE, Rao M, Ferris CD, and Snyder SH. (2002) Biliverdin reductase: a major physiologic cytoprotectant. *Proc Natl Acad Sci USA* **99:** 16093-16098.

Beckman JS, and Koppenol WH (1996) Nitric oxide, superoxide, and peroxynitrite: the good, the bad, and ugly. *Am J Physiol* **271:** C1424-C1437.

Beckman KB, and Ames BN. (1997) Oxidative decay of DNA. *J Biol Chem* **272:** 19633-19636.

Bellner L, Martinelli L, Halilovic A, Patil K, Puri N, Dunn MW, Regan RF, and Schwartzman ML. (2009) Heme oxygenase-2 deletion causes endothelial cell activation marked by oxidative stress, inflammation, and angiogenesis. *J Pharmacol Exp Ther* **331:** 925-32.

Berlett BS, and Stadtman ER. (1997) Protein oxidation in aging, disease, and oxidative stress. *J Biol Chem* **272:** 20313-20316.

Davies KJ (1995) Oxidative stress: the paradox of aerobic life. *Biochem Soc Symp* **61:** 1-31.

Doi K, Akaike T, Fujii S, Tanaka S, Ikebe N, Beppu T, Shibahara S, Ogawa M, and Maeda H. (1999) Induction of haem oxygenase-1 nitric oxide and ischaemia in experimental solid tumours and implications for tumour growth. *Br J Cancer* **80:** 1945-1954.

Duncan R. (2003) The dawning era of polymer therapeutics. *Nat Rev Drug Discov* **2:** 347-360.

Fang J, Akaike T, and Maeda H. (2004) Antiapoptotic role of heme oxygenase (HO) and the potential of HO as a target in anticancer treatment. *Apoptosis* **9:** 27-35.

Fang J, Iyer AK, Seki T, Nakamura H, Greish K, and Maeda H. (2009b) SMA-copolymer conjugate of AHPP: a polymeric inhibitor of xanthine oxidase with potential antihypertensive effect. *J Control Release* **135:** 211-217.

Fang J, Nakamura H, and Maeda H. (2011) The EPR effect: unique features of tumor blood vessels for drug delivery, factors involved, and limitations and augmentation of the effect. *Adv Drug Deliv Rev* **63:** 136-151.

Fang J, Sawa T, Akaike T, Akuta T, Sahoo SK, Khaled G, Hamada A, and Maeda H. (2003) In vivo antitumor activity of pegylated zinc protoporphyrin: targeted inhibition of heme oxygenase in solid tumor. *Cancer Res* **63:** 3567-3574.

Fang J, Seki T, and Maeda H. (2009a) Therapeutic strategies by modulating oxygen stress in cancer and inflammation. *Adv Drug Deliv Rev* **61:** 290-302.

Fang J, Seki T, Qin H, Bharate GY, Iyer AK, and Maeda H. (2010) Tissue protective effect of xanthine oxidase inhibitor, polymer conjugate of (styrene-maleic acid copolymer) and (4-amino-6-hydroxypyrazolo[3,4-*d*]pyrimidine), on hepatic ischemia-reperfusion injury. *Exp Bio Med* **235:** 487-496.

Halliwell B, and Gutteridge JM. (1984) Free radicals, lipid peroxidation, and cell damage. *Lancet* **2:** 1095.

Ikebe N, Akaike T, Miyamoto Y, Hayashida K, Yoshitake J, Ogawa M, and Maeda H. (2000) Protective effect of *S*-nitrosylated α_1-protease inhibitor on hepatic ischemia-reperfusion injury. *J Pharmacol Exp Ther* **295:** 904-911.

Iyer AK, Greish K, Fang J, Murakami R, and Maeda H. (2007) High-loading nanosized

micelles of copoly(styrene-maleic acid)-zinc protoporphyrin for targeted delivery of a potent heme oxygenase inhibitor. *Biomaterials* **28:** 1871-1881.

Jeney V, Balla J, Yachie A, Varga Z, Vercellotti GM, Eaton JW, and Balla G. (2002) Pro-oxidant and cytotoxic effects of circulating heme. *Blood* **100:** 879-887.

Maeda H. (2010) Tumor-selective delivery of macromolecular drugs via the EPR effect: background and future prospects. *Bioconjug Chem* **21:** 797-802.

Maeda H, and Akaike T. (1991) Oxygen free radicals as pathogenic molecules in viral diseases. *Proc Soc Exp Biol Med* **198:** 721-727.

Maeda H, Sawa T, and Konno T. (2001) Mechanism of tumor-targeted delivery of macromolecular drugs, including the EPR effect in solid tumor and clinical overview of the prototype polymeric drug SMANCS. *J Control Release* **74:** 47-61.

Maeda H, Wu J, Sawa T, Matsumura Y, and Hori K. (2000) Tumor vascular permeability and

the EPR effect in macromolecular therapeutics: a review. *J Control Release* **65:** 271-284.

Maines MD. (1988) Heme oxygenase: function, multiplicity, regulatory mechanisms, and clinical applications. *FASEB J* **2:** 2557-2568.

Maines MD, Eke BC, and Zhao X. (1996) Corticosterone promotes increased heme oxygenase-2 protein and transcript expression in the newborn rat brain. *Brain Res* **722:** 83-94.

Matsumura Y, and Maeda H. (1986) A new concept for macromolecular therapeutics in cancer chemotherapy: mechanism of tumoritropic accumulation of proteins and the antitumor agent SMANCS. *Cancer Res* **46:** 6387-6392.

McCord JM. (1985) Oxygen-derived free radicals in postischemic tissue injury. *N Engl J Med* **312:** 159-163.

McCord JM. (2000) The evolution of free radicals and oxidative stress. *Am J Med* **108:** 652-659.

Melgarejo E, Medina MA, Sánchez-Jiménez F, and Urdiales JL. (2009) Monocyte chemoattractant protein-1: a key mediator in inflammatory processes. *Int J Biochem Cell Biol* **41:** 998-1001.

Miyamoto Y, Akaike T, Yoshida M, Goto S, Horie H, and Maeda H. (1996) Potentiation of nitric oxide-mediated vasorelaxation by xanthine oxidase inhibitors. *Proc Soc Exp Biol Med* **211:** 366-373.

Muzykantov VR, Atochina EN, Ischiropoulos H, Danilov SM, and Fisher AB. (1996) Immunotargeting of antioxidant enzyme to the pulmonary endothelium. *Proc Natl Acad Sci USA* **93:** 5213-5218.

Nagamitsu A, Greish K, and Maeda H. (2009) Elevating blood pressure as a strategy to increase tumor-targeted delivery of macromolecular drug SMANCS: cases of advanced solid tumors. *Jpn J Clin Oncol* **39:** 756-766.

Oda T, Akaike T, Hamamoto T, Suzuki F, Hirano T, and Maeda H. (1989) Oxygen radicals in influenza-induced pathogenesis and treatment with pyran polymer-conjugated SOD. *Science* **244:** 974-976.

Ohkawa H, Ohishi N, and Yagi K. (1979) Assay for lipid peroxides in animal tissues by thiobarbituric acid reaction. *Anal Biochem* **95:** 351-358.

Roy RS, and McCord JM. (1983) Superoxide and ischemia: conversion of xanthine dehydrogenase to xanthine oxidase, in *Oxyradicals and Their Scavenger Systems* (Greenwald R, and Cohen G eds) pp 145-153, Elsevier Science, New York.

Sahoo SK, Sawa T, Fang J, Tanaka S, Miyamoto Y, Akaike T, and Maeda H. (2002) Pegylated zinc protoporphyrin: a water-soluble heme oxygenase inhibitor with tumor-targeting capacity. *Bioconjug Chem* **13:** 1031-1038.

Sawa T, Wu J, Akaike T, and Maeda H. (2000) Tumor-targeting chemotherapy by a xanthine oxidase-polymer conjugate that generates oxygen-free radicals in tumor tissue. *Cancer Res* **60:**

666-671.

Seta F, Bellner L, Rezzani R, Regan RF, Dunn MW, Abraham NG, Gronert K, and Laniado-Schwartzman M. (2006) Heme oxygenase-2 is a critical determinant for execution of an acute inflammatory and reparative response. *Am J Pathol* **169:**1612-23.

Stocks SJ, Jones AJ, Ramey CW, and Brooks DE. (1986) A fluorometric assay of the degree of modification of protein primary amines with polyethylene glycol. *Anal Biochem* **154:** 232-234.

Wei Y, Chen P, de Bruyn M, Zhang W, Bremer E, and Helfrich W. (2010) Carbon monoxide-releasing molecule-2 (CORM-2) attenuates acute hepatic ischemia reperfusion injury in rats. *BMC Gastroenterol* **10:** 42.

Footnotes

This work was supported in part by Grants-in-Aid from the Ministry of Education, Science, Culture, Sports and Technology of Japan (Nos. 17016076 and 20015405) and in part by research funds of the Faculty of Pharmaceutical Sciences at Sojo University.

Part of this work was presented in 37th Annual Meeting & Exposition of the Controlled Release Society (Portland, USA, July 10-14, 2009).

To whom reprint requests should be sent: Jun Fang, Laboratory of Microbilogy and Oncology, Faculty of Pharmaceutical Sciences, Sojo University, Ikeda 4-22-1, Kumamoto 860-0082, Japan. Email: fangjun@ph.sojo-u.ac.jp.

[1]These authors contributed equally to this work.

[2]Current address: Laboratory of Angiogenesis Research, Department of Microbiology, Tumor and Cell Biology (MTC), Karolinska Institute, Nobels väg 16, SE-171 77, Stockholm, Sweden.

JPET Fast Forward. Published on September 2, 2011 as DOI: 10.1124/jpet.111.185348
This article has not been copyedited and formatted. The final version may differ from this version.

Legends for figures

Scheme 1. Synthesis and chemical structure of PEG-hemin. An amino group was introduced into hemin (a, $C_{34}H_{32}ClFeN_4O_4$) by using ethylenediamine, which resulted in bis(ethylenediamino) hemin (b, $C_{38}H_{46}ClFeN_8O_2$), which was pegylated via succinimidyl PEG. The resultant PEG-hemin (c, $CH_3O(CH_2CH_2O)_n$-CO-$CH_2CH_2CH_2$-CO- $C_{38}H_{45}ClFeN_8O_2$) formed micelles (d) in aqueous solutions.

Fig. 1. IR spectra of hemin and PEG-hemin. Amide I (1654 cm^{-1}) and amide II (1542 cm^{-1}) were clearly observed in PEG-hemin, which suggested an amide bond formation between hemin and PEG through bis(ethylenediamino) hemin.

Fig. 2. Apparent molecular mass of PEG-hemin in aqueous solutions as analyzed by Sephadex G-100 gel chromatography (A) and DLS (B). Gel chromatography was performed with the mobile phase of 0.25 M $NaHCO_3$ (pH 8.2), and the molecular mass of PEG-hemin in aqueous solutions was calculated by reference to known molecular mass protein markers. See text for details.

Fig. 3. Pharmacokinetics of PEG-hemin and native hemin in blood of ddY mice. Native hemin or PEG-hemin was injected i.v. into ddY mice via the tail vein. After scheduled intervals, mice were killed, blood was collected, and blood concentrations of hemin and PEG-hemin were measured as described in "Materials and methods". Values are means ± SE; $n = 4$. $^{**}P < 0.01$, $^{***}P < 0.001$, PEG-hemin *vs*. native hemin.

Fig. 4. *In vitro* cytotoxicity (A) and HO-1 induction activity (B) of PEG-hemin. The viability of human hepatocytes (Hc) was determined by using the MTT assay. Values are means ± SE; $n = 8$ wells. See text for details.

Fig. 5. *In vivo* induction of HO-1 by PEG-hemin in a rat I/R model. Western blot for HO-1 protein in liver tissue (A) and HO-1 activity, as evidenced by bilirubin formation, in liver tissue after I/R with or without PEG-hemin treatment (B). HO-1 induction was further verified by measuring the CO concentration in blood (C). See text for details. All data are presented as means ± SE; $n = 4$. $^{*}P < 0.05$, $^{**}P < 0.01$.

Fig. 6. Effect of PEG-hemin on hepatic I/R injury evaluated by changes in serum levels of

AST, ALT, and LDH (A), and histological examination of rat liver tissue (B). Ischemia was induced by occluding both the portal vein and hepatic artery for 30 min followed by reperfusion for 3 h. PEG-hemin (PH) was administered i.v. 2 h before ischemia. The concentration of SMA-ZnPP administered to rats was 5 mg/kg. See text for details. Data are presented as means ± SE; n = 3-12. *P < 0.05, **P < 0.01. Arrows in B indicate necrotic areas of liver tissue.

Fig. 7. Time profile of changes in hepatic blood flow before and after I/R and PEG-hemin treatment. Blood flow values are expressed as a percentage of the value measured before ischemia. PEG-hemin (10 mg/kg) was injected i.v. as noted in Fig. 6. Data are presented as means ± SE; n = 3-4. *P < 0.05, **P < 0.01, PEG-hemin *vs*. native hemin.

Fig. 8. Effect of PEG-hemin on I/R-induced apoptotic changes in the liver. Rats were treated with PEG-hemin before I/R, as given in Fig. 6. At 3 h after reperfusion, liver tissues were collected and paraffin-embedded sections were prepared for TUNEL staining (A). The caspase 3/7 activities in the liver tissues were also quantified (B). Arrows point to apoptotic cells (A). Data are presented as means ± SE; n = 3-6. *P < 0.05, **P < 0.01.

Fig. 9. TBARS and 8-OHdG in the rat liver after I/R injury with or without PEG-hemin treatment. The experimental protocol is the same as that noted in Fig. 6. At 3 h after reperfusion, rats were killed and the liver tissues were collected and subjected to the TBARS assay and ELISA assay of 8-OHdG (See "Materials and methods" for details). Data are presented as means ± SE; n = 3-4. *$P < 0.05$.

Fig. 10. Induction of MCP-1 by I/R injury and the protective effect of PEG-hemin. I/R and treatment protocols were the same as mentioned in Fig. 6. The serum MCP-1 concentration was measured by using an ELISA kit. Data are presented as means ± SE; n = 4-6. *$P <$ 0.05.

JPET Fast Forward. Published on September 2, 2011 as DOI: 10.1124/jpet.111.185348
This article has not been copyedited and formatted. The final version may differ from this version.

Table 1.

Pharmacokinetic parameters of free hemin and PEG-hemin

Agent	**$t_{1/2}$ (h)[a]**	**AUC[b] (μg/ml/h)**	**Total body clearance (L/h/kg)**
Hemin	0.96	203.3	49.2
PEG-hemin	18.25	3289.3	3.0

[a]Plasma $t_{1/2}$ required to reach to half-concentration at time zero by interpolation.

[b]Area under the plasma concentration *vs.* time curve.

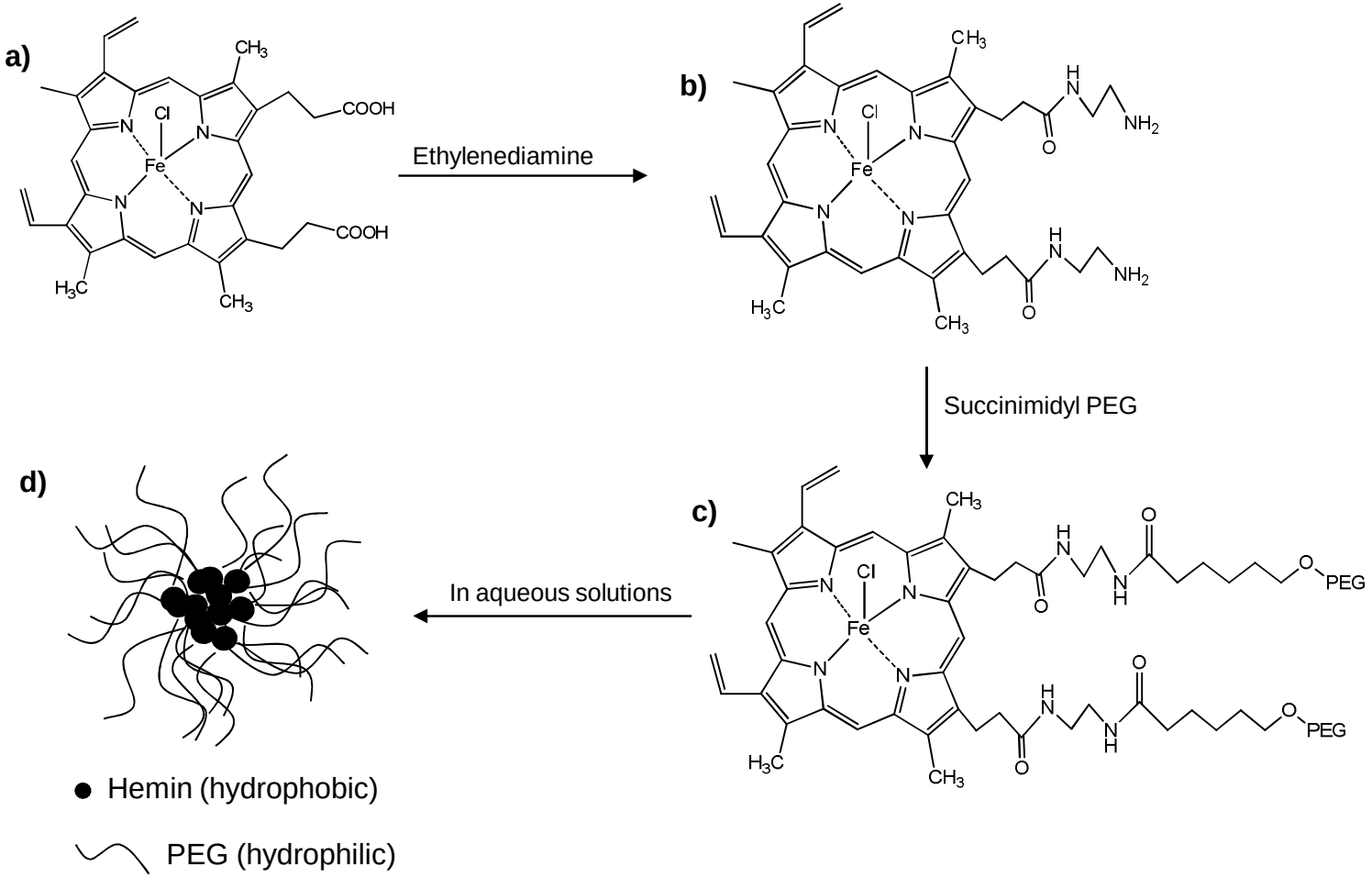

Fig. 1

top ↑

JPET #185348

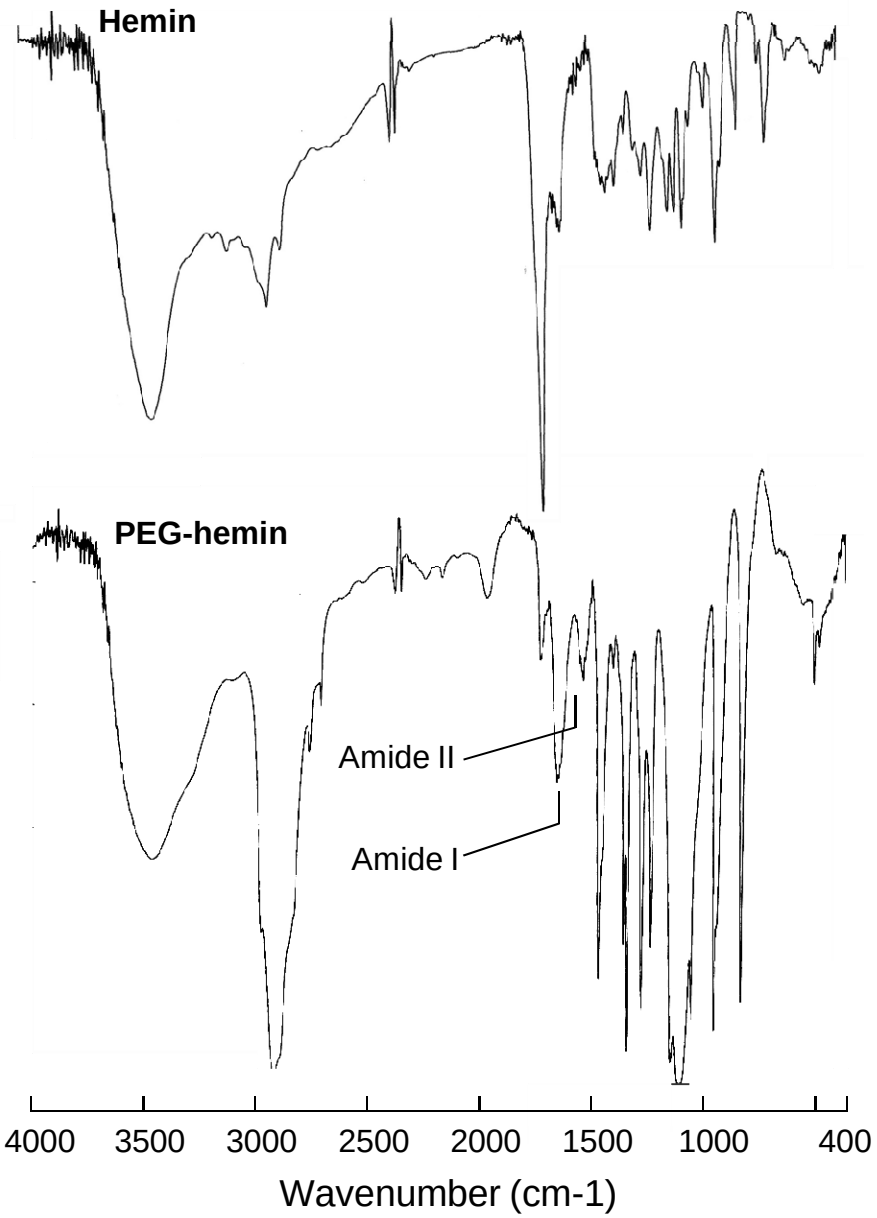

Fig. 2

top ↑

JPET #185348

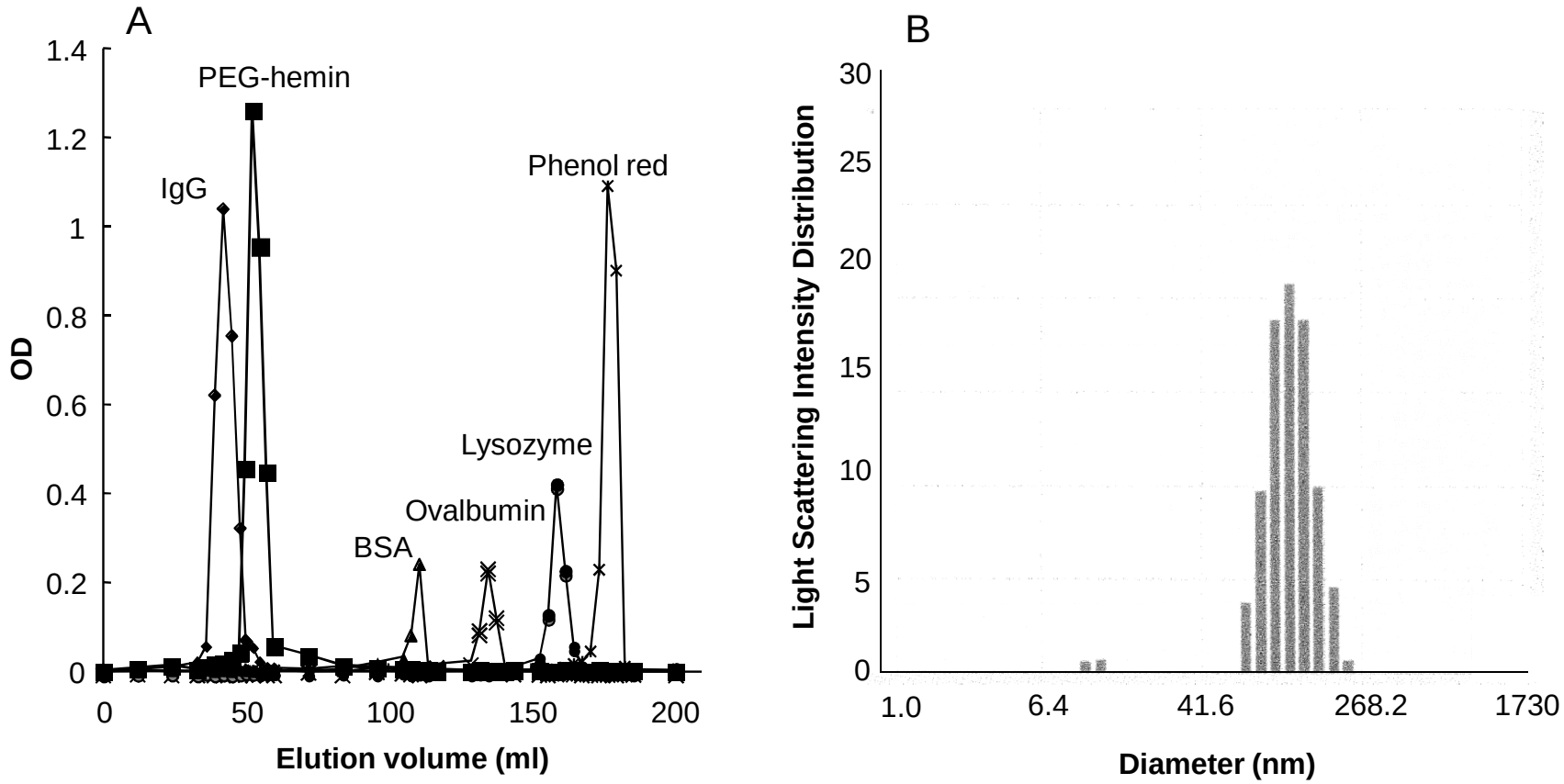

Fig. 3

top ↑

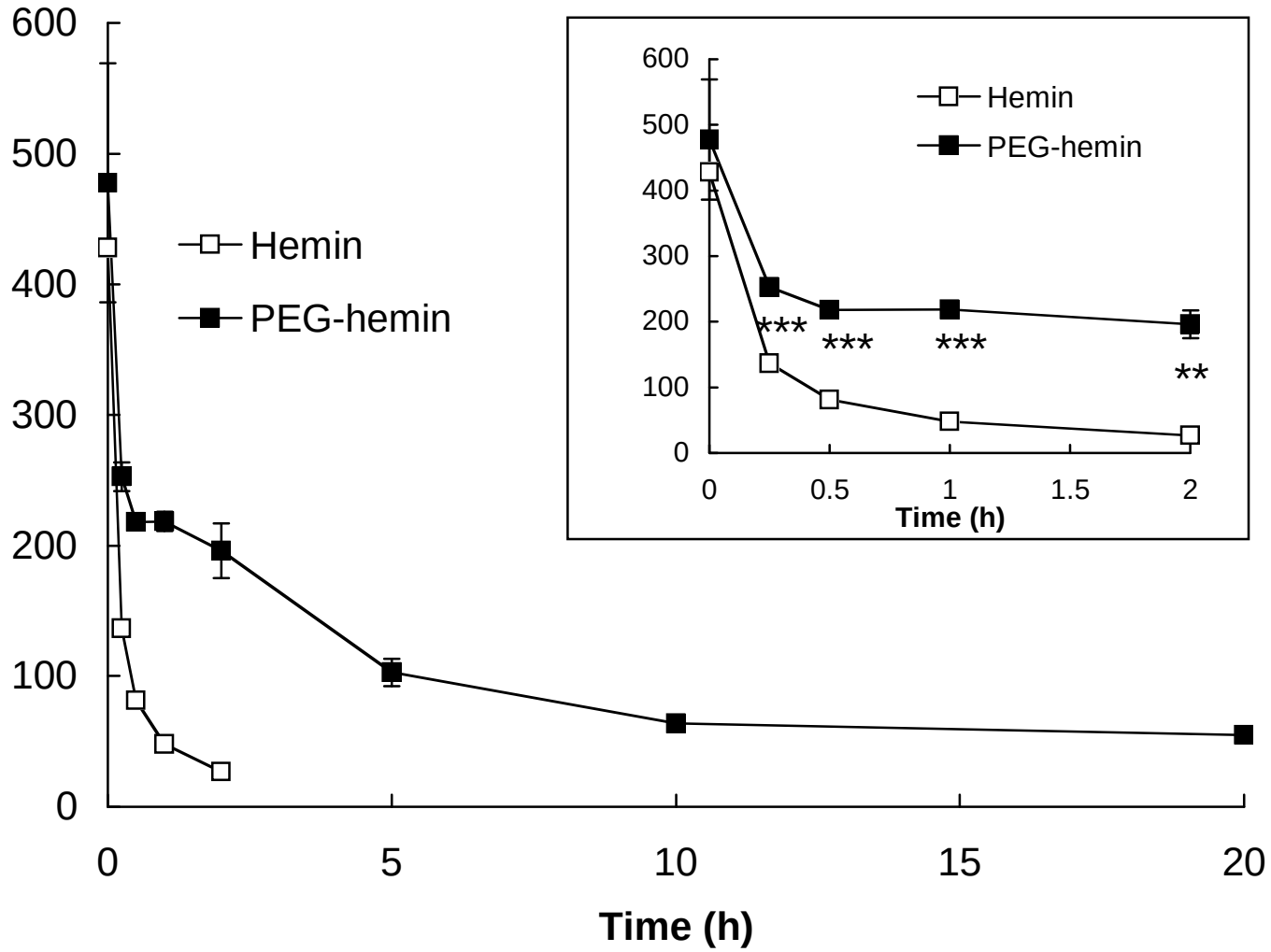

Fig. 4 top ↑ JPET #185348

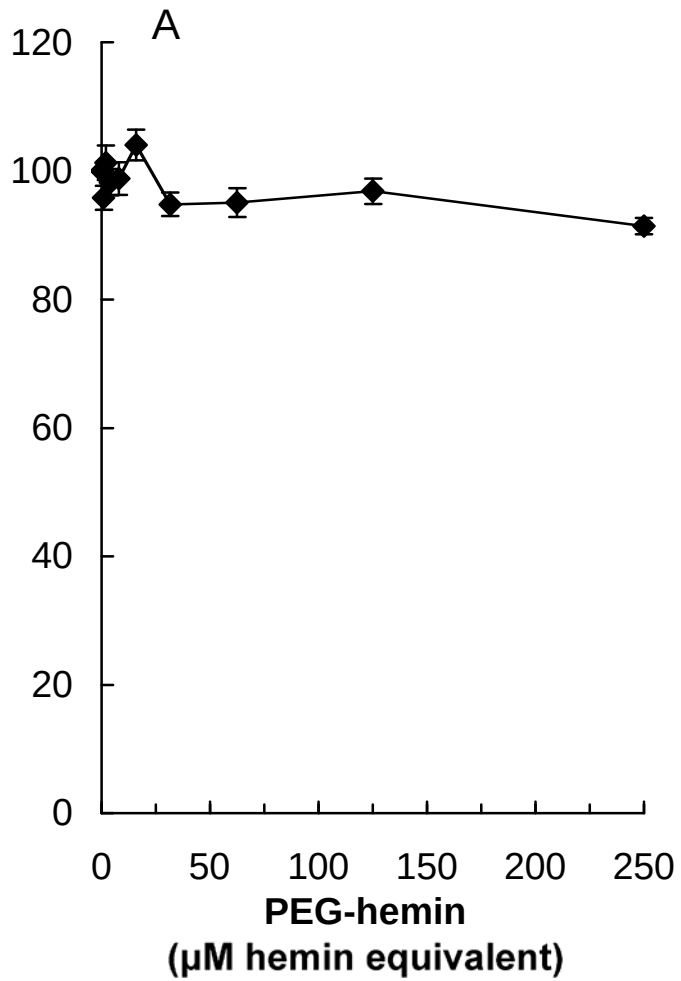

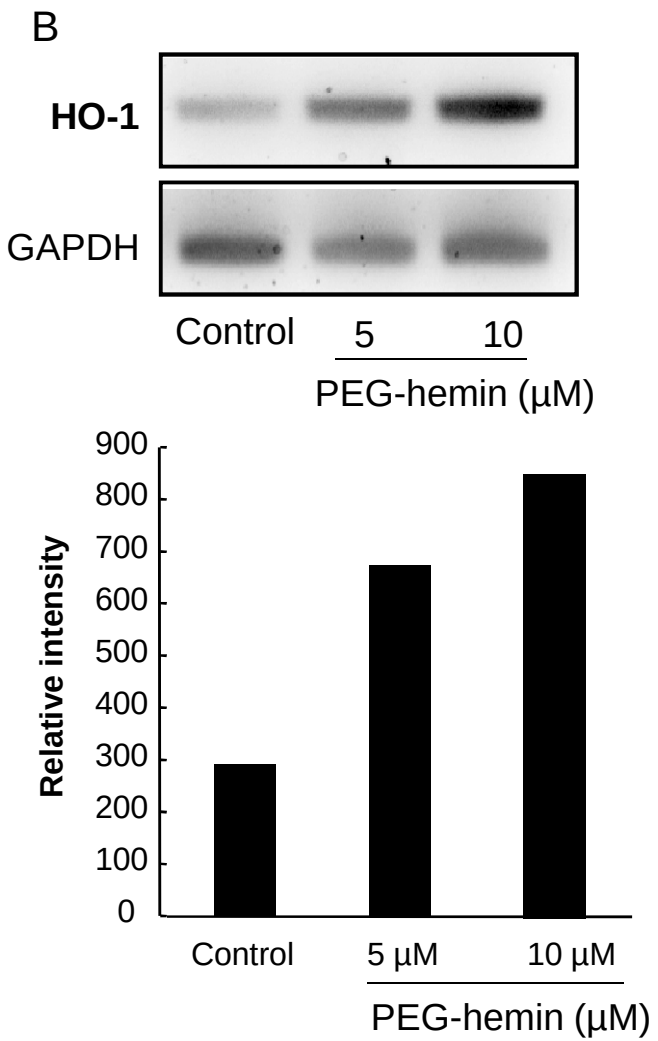

Fig. 5 top ↑ JPET #185348

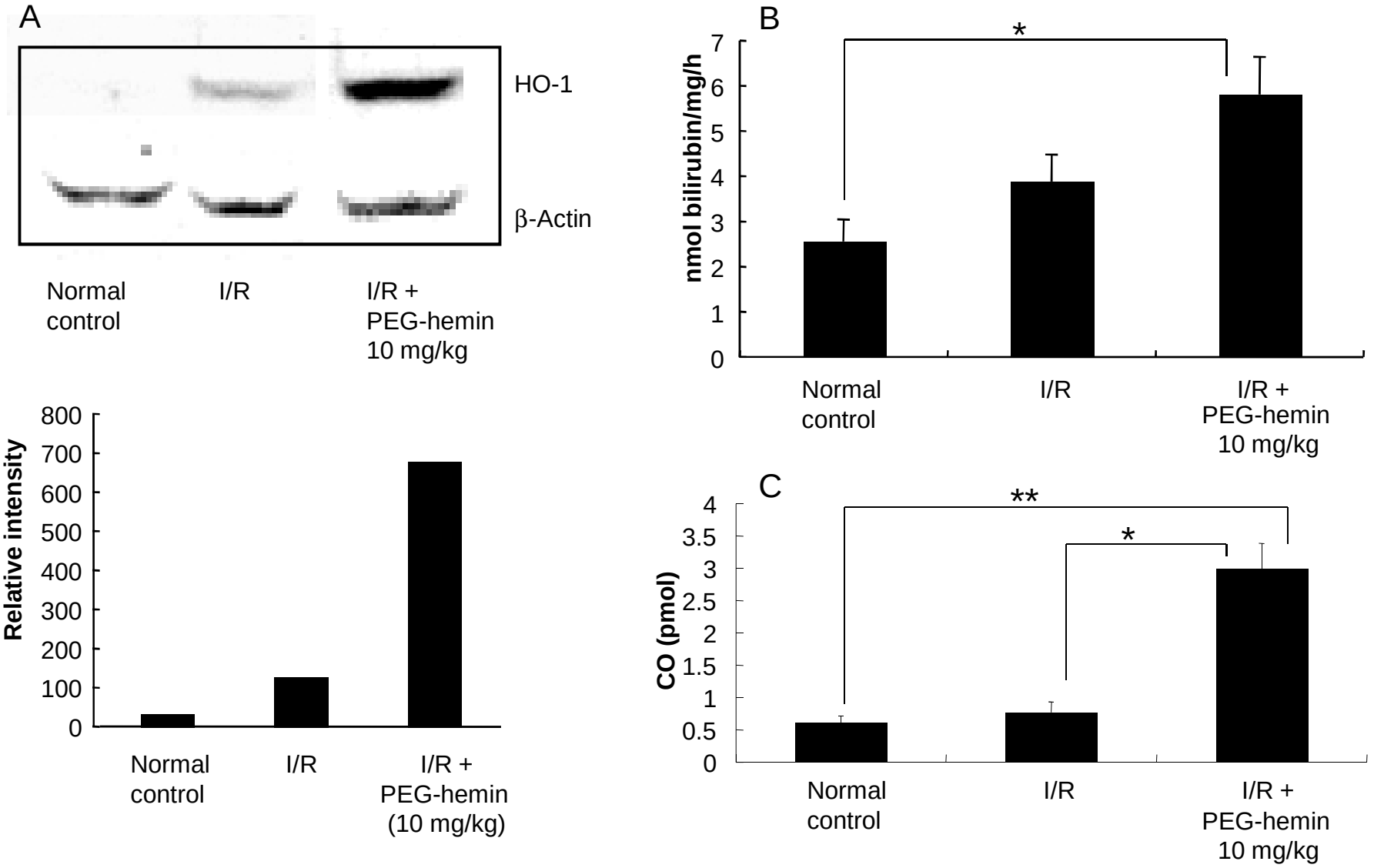

Fig. 6

top ↑

JPET #185348

A

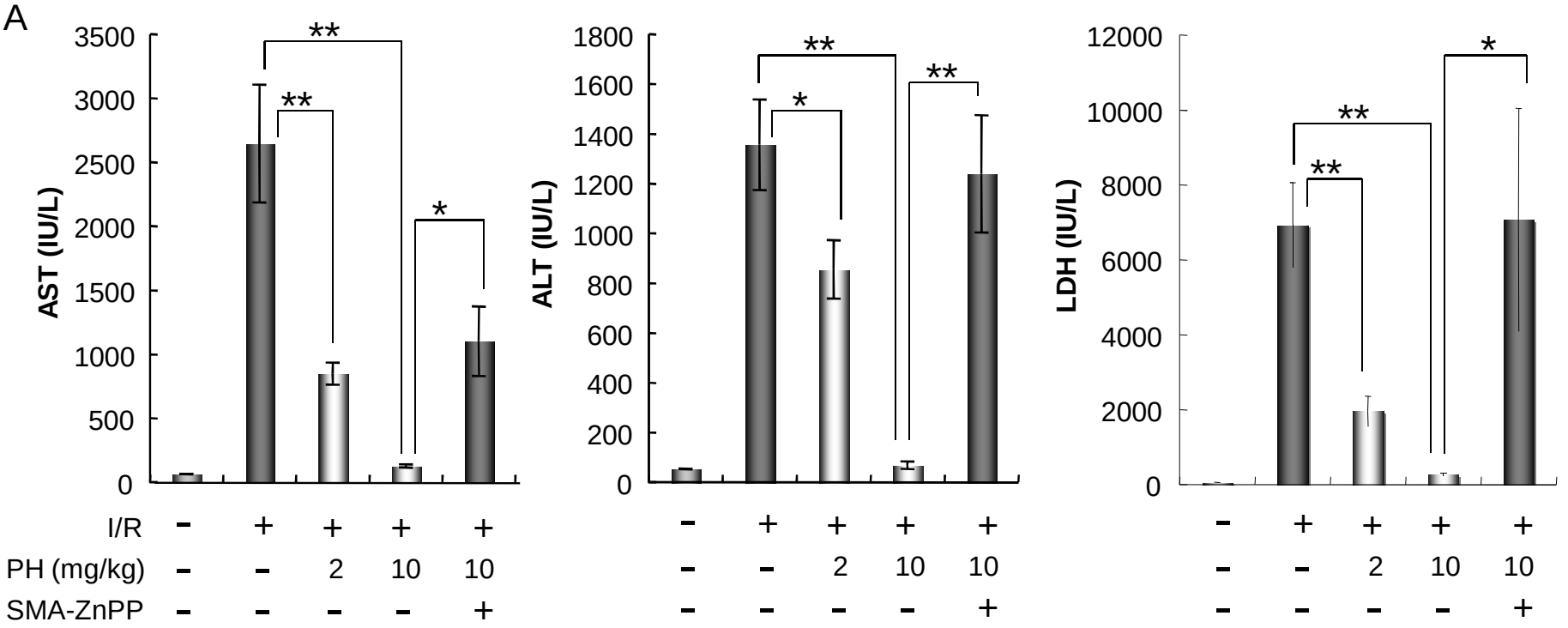

B

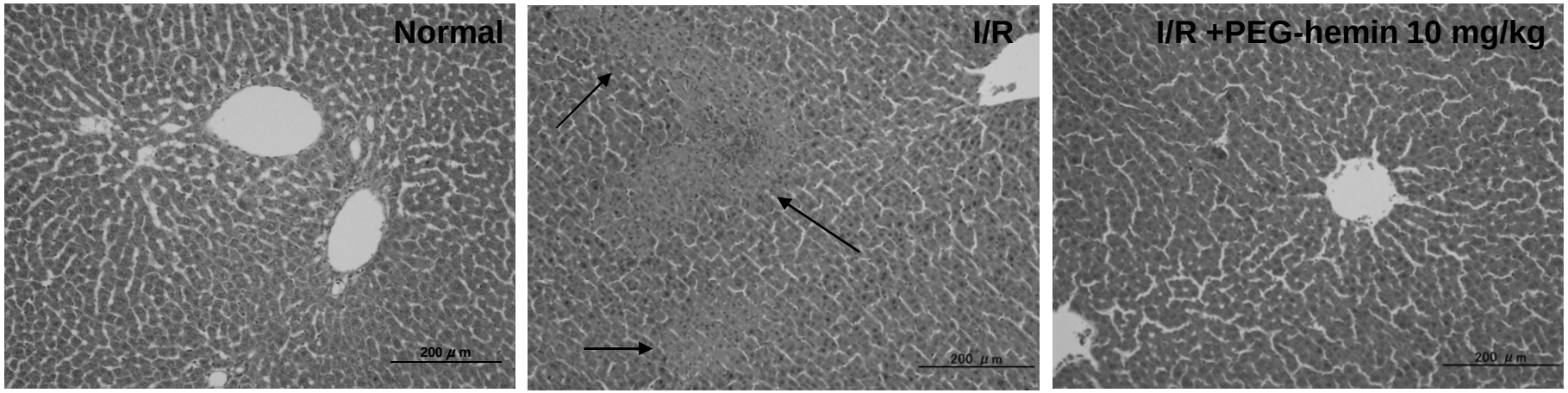

Fig. 7 top ↑ JPET #185348

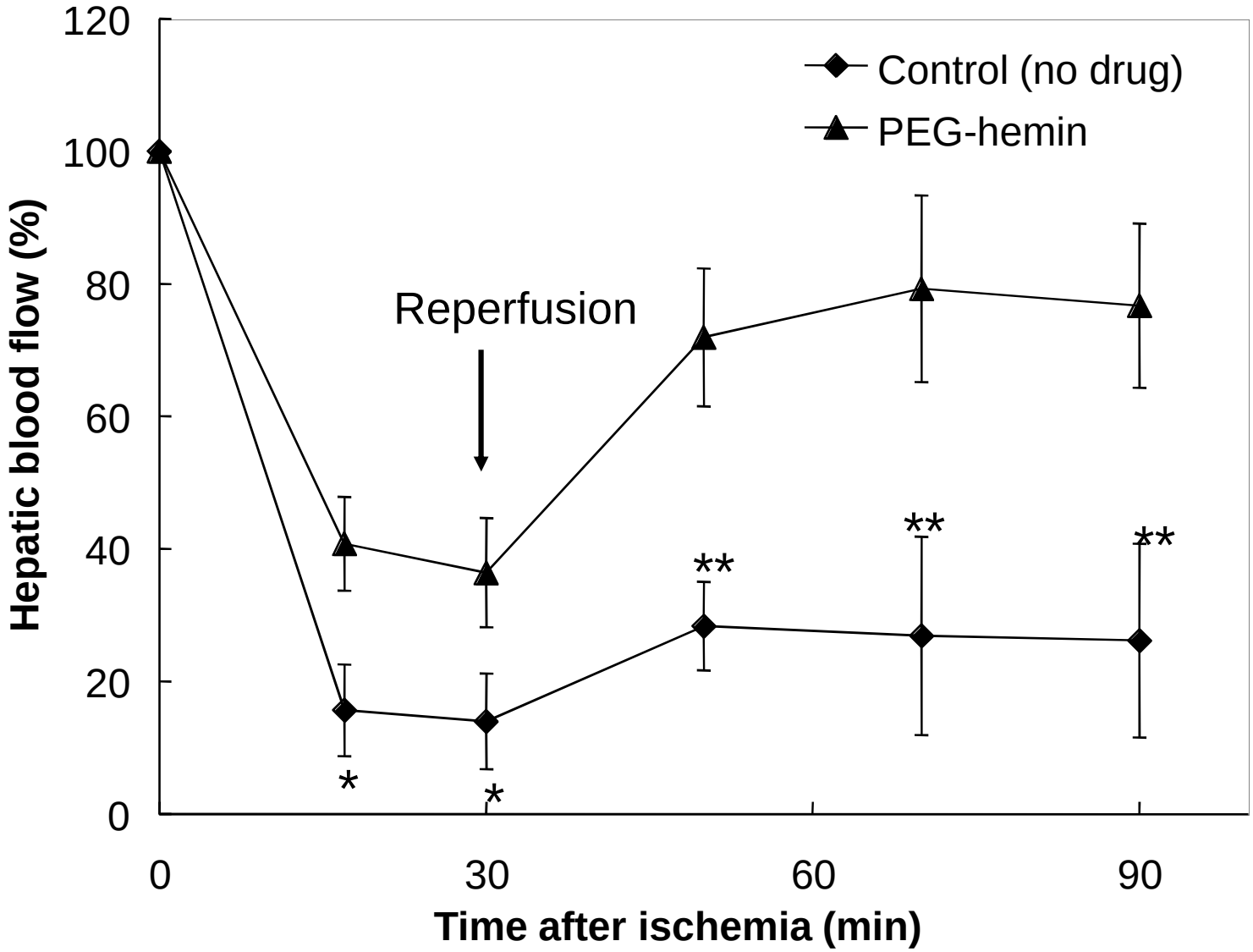

Fig. 8 top ↑ JPET #185348

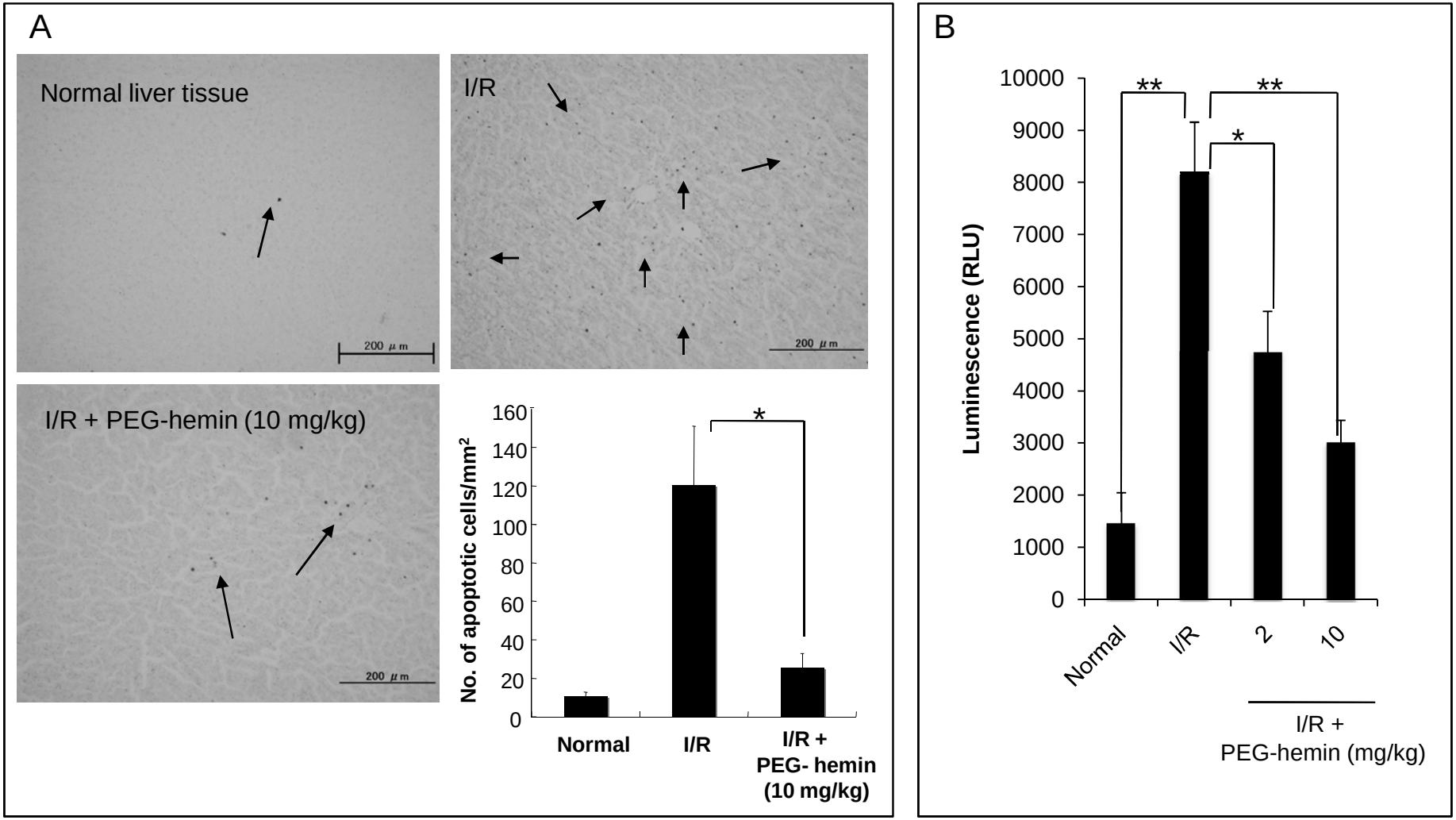

Fig. 9

top ↑

JPET #185348

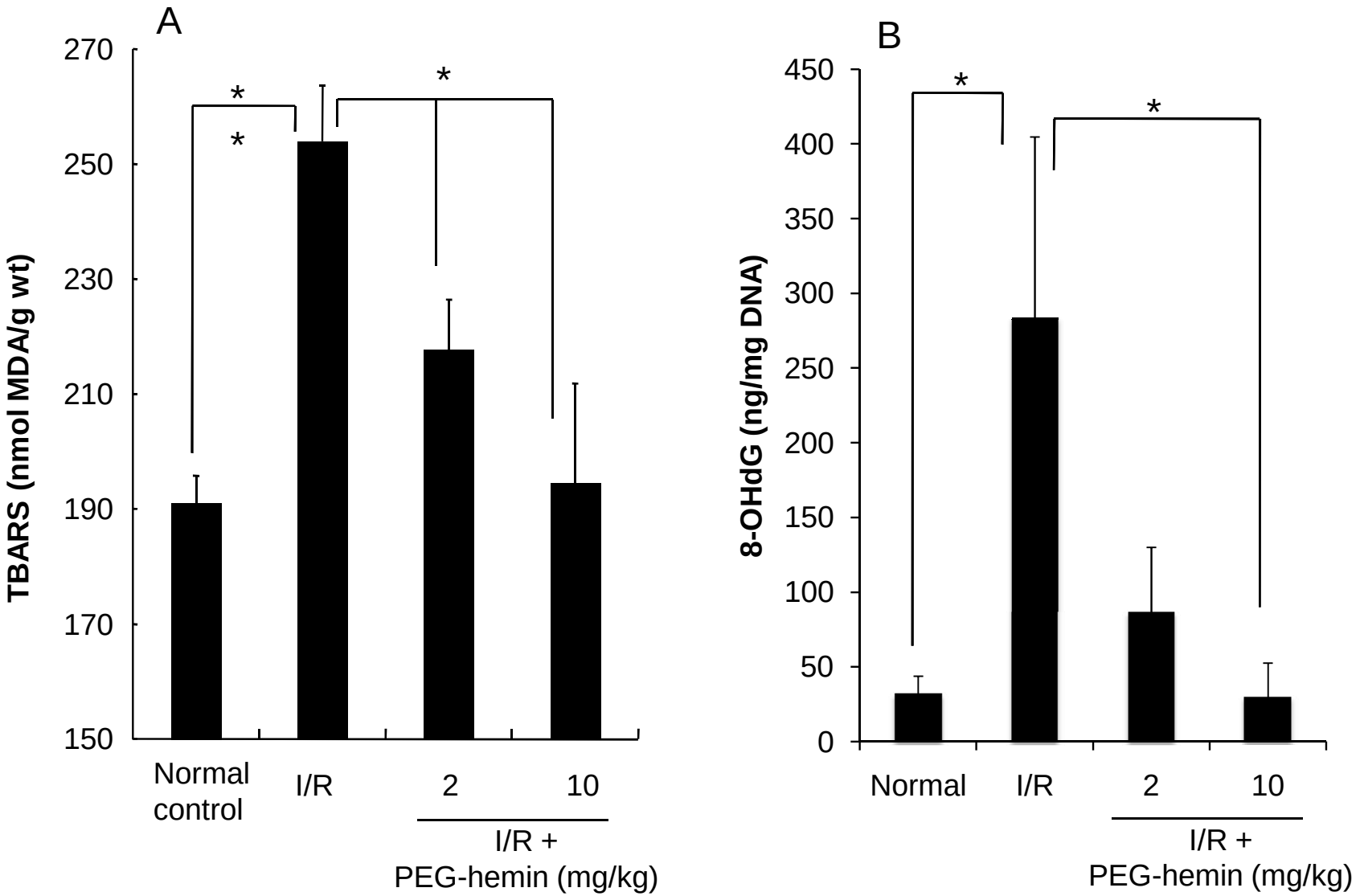

Fig. 10

top ↑

JPET #185348